ORIGINAL ARTICLES

Bile-acid-activated farnesoid X receptor regulates hydrogen sulfide production and hepatic microcirculation

Barbara Renga, Andrea Mencarelli, Marco Migliorati, Eleonora Distrutti, Stefano Fiorucci

Barbara Renga, Andrea Mencarelli, Marco Migliorati, Stefano Fiorucci, Department of Clinical and Experimental Medicine, University of Perugia, Via E dal Pozzo, 06122 Perugia, Italy

Eleonora Distrutti, Azienda Ospedaliera di Perugia, Ospedale Santa Maria della Misericordia, 06122 Perugia, Italy

Author contributions: Renga B designed the study, carried out *in vitro* experiments and wrote the manuscript; Migliorati M performed *in vitro* experiments (Western blotting and PCR); Mencarelli A performed *in vivo* experiments; Distrutti E was involved in designing and writing the manuscript; Fiorucci S designed the study and wrote the manuscript.

Correspondence to: Barbara Renga, Department of Clinical and Experimental Medicine University of Perugia, Via E dal Pozzo, 06122 Perugia, Italy. barbara.renga@unipg.it

Telephone: +39-075-5855819 Fax: +39-075-5855819

Received: December 19, 2008 Revised: March 20, 2009

Accepted: March 27, 2009

Published online: May 7, 2009

Abstract

AIM: To investigate whether the farnesoid X receptor (FXR) regulates expression of liver cystathionase (CSE), a gene involved in hydrogen sulfide (H_2S) generation.

METHODS: The regulation of CSE expression in response to FXR ligands was evaluated in HepG2 cells and in wild-type and FXR null mice treated with 6-ethyl chenodeoxycholic acid (6E-CDCA), a synthetic FXR ligand. The analysis demonstrated an FXR responsive element in the 5′-flanking region of the human *CSE* gene. The function of this site was investigated by luciferase reporter assays, chromatin immunoprecipitation and electrophoretic mobility shift assays. Livers obtained from rats treated with carbon tetrachloride alone, or in combination with 6-ethyl chenodeoxycholic acid, were studied for hydrogen sulphide generation and portal pressure measurement.

RESULTS: Liver expression of CSE is regulated by bile acids by means of an FXR-mediated mechanism. Western blotting, qualitative and quantitative polymerase chain reaction, as well as immunohistochemical analysis, showed that expression of CSE in HepG2 cells and in mice is induced by treatment with an FXR ligand. Administration of 6E-CDCA to carbon tetrachloride treated rats protected against the down-regulation of CSE expression, increased H_2S generation, reduced portal pressure and attenuated the endothelial dysfunction of isolated and perfused cirrhotic rat livers.

CONCLUSION: These results demonstrate that CSE is an FXR-regulated gene and provide a new molecular explanation for the pathophysiology of portal hypertension.

Renga B, Mencarelli A, Migliorati M, Distrutti E, Fiorucci S. Bile-acid-activated farnesoid X receptor regulates hydrogen sulfide production and hepatic microcirculation. *World J Gastroenterol* 2009; 15(17): 2097-2108 Available from: URL: http://www.wjgnet.com/1007-9327/15/2097.asp DOI: http://dx.doi.org/10.3748/wjg.15.2097

INTRODUCTION

In mammals, cysteine is provided through the diet or by the trans-sulfuration pathway, in which L-cysteine is synthesized by sulfur transfer from L-methionine to L-serine. Cystathionine-γ-lyase (CSE) is a pyridoxal 5'-phosphate-dependent enzyme, which catalyze the final essential step of the trans-sulfuration pathway; the conversion of L-cystathionine into L-cysteine, α-ketobutyrate and ammonia[1-3]. Cysteine is further irreversibly metabolized in the liver to yield glutathione[4-6], taurine[7] and hydrogen sulfide (H_2S), a gaseous bioactive molecule[3,8]. CSE is the main enzyme involved in H_2S generation by vascular smooth muscle cells[9,10] and accounts for the vasodilatory effect of H_2S in the systemic circulation[11,12]. In the liver, H_2S generated by hepatocytes and hepatic stellate cells exerts vasodilatory activities and reduces intrahepatic resistance counter-acting the effect of vasomotor mediators on presinusoidal myofibroblasts[13,14].

An alteration of the trans-sulfuration pathway is common in chronic liver diseases, with hyper-homocysteinemia occurring in two-thirds of cirrhotic

patients, regardless the etiology of liver damage[15,16]. An imbalance of the trans-sulfuration pathway linked to reduced expression and activity of CSE is observed in rodent models of liver injury. This alteration leads to a combination of hyper-homocysteinemia and reduced generation of H_2S, translating into an enhanced vasomotor tone and increased intrahepatic resistance[17,18]. Homocysteine is a negative regulator of nitric oxide (NO) bioactivity in endothelial cells. Perfusion of the normal and cirrhotic rat livers with homocysteine results in attenuated NO generation and impaired hepatic vasodilation in response to acetylcholine and shear stress, highlighting the critical role of intermediates of the trans-sulfuration pathway in regulating intrahepatic vasomotor activity[18].

Little is known about the mechanism responsible for the reduced expression of CSE in the injured liver. The fact that CSE expression is modulated during development, being detected at very low levels in embryos while a gradual increase of expression occurs after birth, suggests that genes involved in liver differentiation or proliferation might control the expression of this gene[1].

The farnesoid X receptor (FXR, NR1H4), a member of the ligand-activated nuclear hormone receptor superfamily, is primarily expressed in the liver, kidney, and intestine[19]. It functions as a heterodimer with the retinoid X receptor (RXR)[20] and binds to response elements in the promoters of target genes involved in bile acid homeostasis, and lipid and glucose metabolism[21]. The FXR-RXR heterodimer binds with highest affinity to an inverted repeat sequence in which consensus receptor-binding hexamers are separated by one nucleotide (IR1: AGGTCAgTGACCT)[22]. FXR functions as a bile acid sensor, and upon activation, it reduces the conversion of cholesterol into bile acids and increase bile acid excretion from hepatocytes by activating canalicular transporters. In the present study, we investigated whether FXR regulates H_2S generation. Our results demonstrate that the 5'-flanking region of the human *CSE* gene contains an FXR response element (AGTTCAgTGTACCT) and that FXR activation *in vitro* and *in vivo* enhances CSE expression and activity, and directly stimulates H_2S generation. These data suggest that FXR directly regulates the generation of a vasodilatory mediator in the liver and provide new pathophysiological insights into the molecular mechanism of portal hypertension.

MATERIALS AND METHODS

Cell culture
HepG2 cells were grown at 37℃ in Minimum Essential Medium with Earl's salts containing 10% fetal bovine serum (FBS), 1% L-glutamine and 1% penicillin/streptomycin. Cells were serum starved for 24 h and then stimulated with 6E-CDCA (6-ethyl-chenodexycholic acid) 10 μmol/L for 18 h. At the end of treatment, total RNA and proteins were extracted to investigate the expression of CSE. Cells were also fixed in acetone and

stained with a CSE monoclonal antibody (provided by Dr. N. Nishi, Kagawa Medical School, Japan)[19].

RNA extraction
Total RNA was isolated from liver or HepG2 cells using the TRIzol reagent according to the manufacturer's specifications (Invitrogen, Milan, Italy). One microgram of RNA was purified from genomic DNA by DNase- I treatment (Invitrogen) and reverse-transcribed using random hexamer primers with Superscript Ⅱ (Invitrogen) in a 20-μL reaction volume.

Qualitative and quantitative real-time polymerase chain reaction (RT-PCR)
The amplification of cDNA (50 ng) was achieved in a 50-μL mixture containing 200 nmol/L dNTPs, 1.5 mmol/L MgCl$_2$, 200 nmol/L gene-specific sense and antisense primers and 1 U Platinum *Taq* DNA Polymerase (Invitrogen). All PCR primers were designed using software PRIMER3-OUTPUT using published sequence data from the NCBI database (Table 1). Quantitative RT-PCR conditions were as described previously[13].

Western blotting anti-CSE
Total lysates were prepared by solubilization of cells or liver homogenates in NuPage sample buffer (Invitrogen) containing Sample Reducing Agent (Invitrogen) and separated by PAGE. The proteins were then transferred to nitrocellulose membranes (Bio-Rad) and probed with primary antibodies CSE[17,23] and tubulin (Sigma). The anti-immunoglobulin G horseradish peroxidase conjugate (Bio-Rad) was used as the secondary antibody, and specific protein bands were visualized using Super Signal West Dura (Pierce), following the manufacturer's suggested protocol.

Immunohistochemical analysis of CSE
Immunohistochemical analysis of CSE was performed in HepG2 cells and in liver sections from FXR +/+ and FXR -/- mice not treated and treated with CCl$_4$. Cells were fixed in 95% acetone for 5 min and endogenous peroxidase was blocked using Dako Peroxide Blocking (DAKO) for 10 min. An anti-CSE monoclonal antibody[23] was used at a dilution of 1:100 for 1 h at room temperature and a biotin-streptavidin-HRP detection/DAB substrate chromogen system was used to visualize the detected proteins. For liver staining, portions of the right and left liver lobes (15 mg/each) from each animal were fixed in 10% formalin, embedded in paraffin, sectioned, blocked with Dako Peroxide Blocking and stained with CSE monoclonal antibody diluted 1:100 for 1 h at room temperature. A biotin-streptavidin-HRP detection system was used using DAB substrate as the chromogen.

Measurement of CSE activity
The CSE activity was assessed accordingly to the method reported by Ogasawara *et al*[24] with minor modifications;

Table 1 Primers used for quantitative and qualitative PCR

Gene	Forward	Reverse
hGAPDH	GAAGGTGAAGGTCGGAGT	CATGGGTGGAATCATATTGGAA
hCSE	CACTGTCCACCACGTTCAAG	GTGGCTGCTAAACCTGAAGC
hCSE-IR1	CATTACAGAGTTCAGTGTACCT	GCAGCTTGGATTCTCATCAGTC
r18S	GCAATTATTCCCCATGAACG	GGCCTCACTAAACCATCCAA
rCSE	GTATTGAGGCACCAACAGGT	GTTGGGTTTGTGGGTGTTTC
rFXR	TGGACTCATACAGCAAACAGAGA	GTCTGAAACCCTGGAAGTCTTTT
rαSMA	GCTCCATCCTGGCTTCTCTA	TAGAAGCATTTGCGGTGGAC
rCOL1α1	TGCTGCCTTTTCTGTTCCTT	GGATTTGAAGGTGCTGGGTA
rSHP	CCTGGAGCAGCCCTCGTCTCAG	AACACTGTATGCAAACCGAGGA
m18S	ACCGCAGCTAGGAATAATGGA	GCCTCAGTTCCGAAAACCA
mCSE	TGCTGCCACCATTACGATTA	GATGCCACCCTCCTGAAGTA
mα1-collagen	ACGTCCTGGTGAAGTTGGTC	CAGGGAAGCCTCTTTCTCCT

h: Human; m: Mouse; r: Rat; hCSE-IR1: Primers used for real-time PCR of the CSE promoter in chromatin immunoprecipitation assay.

DL-propargylglycine (final 1 mmol/L) instead of 4,4-dithiodipyridine (final 3 mmol/L) was used to inactivate CSE. This method utilizes colorimetry for the determination of pyruvate produced from β-chloro-L-alanine by a CSE-catalyzed elimination reaction, coupling a color-generating enzymatic reaction with pyruvate oxidase and peroxidase. The CSE-specific activity was expressed as the ratio (between sample and sample blank) of absorbance at 727 nm per microgram of protein per seconds of incubation. Sulfide concentrations and production from liver supernatants were measured as previously described[13].

Transactivation assay

For the luciferase assay, 24 h before transfection, 10×10^5 HepG2 cells were plated in six-well plates and cultured in E-MEM supplemented with 1% penicillin/streptomycin, 1% L-glutamine and 10% FBS. Cells were grown at 37℃ in 5% CO2. All the transfections were made using Fugene HD according to manufacturer's specifications (Roche) and performed using 1 μg pGL3 or pGL3 (CSE-IR1)4X or pGL3CSEIR1mutated as reporter vectors, 200 ng pCMV-βgalactosidase as an internal control for transfection efficiency, and 100 ng of each expression plasmid pSG5-FXR and pSG5-RXR. The pGEM vector was added to normalize the amounts of DNA transfected in each assay to 2.5 μg/well. Forty-eight hours post-transfection, HepG2 cells were stimulated with a dose response of 6E-CDCA (from 0.01 to 10 μmol/L) or with bile acids (25 μmol/L) for 18 h. Control cultures received vehicle (0.1% DMSO) alone. For the competition assay, an FXR antagonist, such as guggulsterone, was used at 50 μmol/L alone, or in combination with 6E-CDCA 10 μmol/L, for 18 h. Cells were lysed in 100 μL diluted reporter lysis buffer (Promega), and 5 μL of cellular lysate was assayed for luciferase activity using Luciferase Assay System (Promega). Luminescence was measured using an automated luminometer. Luciferase activities were normalized for transfection efficiencies by dividing the relative light units by β-galactosidase activity. All experiments were done in triplicate and were repeated at least once.

Electrophoretic mobility shift assay (EMSA)

Preparation of nuclear extract from HepG2 cells was done using NE-PER (Pierce). The probes used for EMSA (CSERE-IR1, CSERE-IR1mutated and FXRE-IR1) were labeled with biotin using Biotin 3' end DNA labelling kit (Pierce) according to the manufacturer's instructions. For EMSA, 5 μg of nuclear extract from HepG2 cells not treated or stimulated with 6E-CDCA 10 μmol/L were incubated with 15 fmol of the CSERE-IR1 probe, while 5 μg of nuclear extract from HepG2 stimulated with 6E-CDCA was incubated with CSERE-IR1mutated and FXRE-IR1 probes in a total volume of 20 μL of binding buffer (50 mmol/L NaCl, 10 mmol/L Tris-HCl, pH 7.9, 0.5 mmol/L EDTA, 10% glycerol, 1 μg of poly dI-dC) for 20 min at room temperature. For competition assays, an excess of CSERE-IR1 unlabeled oligonucleotides were pre-incubated with nuclear extract from 6E-CDCA-treated cells for 15 min prior to the addition of the biotin-labeled CSERE-IR1 probe. For antibody-mediated supershift assay, extracts from stimulated cells were pre-incubated with 1 μg anti-FXR antibody H-130 (Santa Cruz Biotechnology, Santa Cruz, CA, USA) or with 1 μg anti-RXR antibody ΔN 197 (Santa Cruz Biotechnology) at room temperature for 20 min before the addition of the biotin-labeled CSERE-IR1 probe. The reactions were loaded on a 6% polyacrylamide non-denaturing gel in 0.5 × Tris-borate-EDTA buffer and electrophoresed for 1 h at 100 V. The protein/DNA complexes were then transferred to positively charged nylon membrane (Pierce) and the supershift was detected using the Chemiluminescent Nucleic Acid Detection Module (Pierce).

Chromatin immunoprecipitation (ChIP)

A ChIP assay was performed according to the manufacturer's protocols (Abcam Ltd, Cambridge, UK) with minor modifications. In brief, HepG2 cells serum starved for 24 h, not treated or stimulated with 6E-CDCA 10 μmol/L for 18 h, were cross-linked with 1% formaldehyde at room temperature, and then the reaction was terminated by the addition of glycine to a final concentration of 0.125 mol/L. Cells were washed in ice-cold PBS and lysed with SDS lysis buffer (1% SDS, 10 mmol/L EDTA, and 50 mmol/L Tris-HCl, pH 8). Cellular lysates were diluted with ChIP dilution buffer, sonicated, and immunoprecipitated with specific

antibodies: anti-FXR or anti-CD4 as a negative control (Santa Cruz Biotechnology). Immunoprecipitates were collected with protein A beads (Amersham Bioscience) and washed sequentially, first with a low-salt wash buffer and then with high-salt wash buffer using the manufacturer's recommended procedures. DNA was eluted by addition of 1% SDS and 0.1 mol/L $NaHCO_3$, and the cross-linking reactions were reversed by heating the mixture to 65℃ overnight. The DNA was recovered from immunoprecipitated material by proteinase K treatment at 65℃ for 1 h followed by phenol/chloroform (1:1) extraction, ethanol precipitation and dissolved into 50 μL of water. Five microliters was used for quantitative real-time PCR. Five microliters of PCR reactions were extracted after 40 complete cycles for visualization on agarose gels and stained with ethidium bromide.

In vivo experimental studies

All animal procedures were approved by the Animal Study Committees of the University of Perugia. In the first study, the effect of FXR ligands on liver expression of CSE was investigated in FXR +/+ and FXR -/- mice treated by intraperitoneal injection of 6E-CDCA 5 mg/kg body weight for 3 d while control animals were treated with vehicle alone (methyl-cellulose). C57BL/6j mice, obtained from Charles River Breeding Laboratories (Monza, Italy), and homozygous C57BL/6j FXR -/- mice, obtained from Gonzalez et al[25] were used with a 12 h light/12 h dark cycle with free access to water and standard laboratory chow diet. At the end of the study, mice were sacrificed and their livers were removed to measure the relative mRNA expression of CSE, the activity of the enzyme and the production of H_2S. In the second study, cirrhosis was induced in FXR +/+ and FXR -/- mice by administering phenobarbital sodium (35 mg/dL) to the mice with drinking water for 3 d, followed by intraperitoneal injection of 100 μL/100 g body weight of CCl_4 in an equal volume of paraffin oil twice 1 wk for 6 wk. CCl_4 administered mice were treated with intraperitoneal injection of 6E-CDCA 5 mg/kg body weight, while control animals were treated with vehicle alone (methyl-cellulose). Mice were sacrificed and their livers were removed for histological, histochemical, and real-time PCR analysis. Blood samples were taken for biochemical analysis. In the third study, cirrhosis was induced in rats obtained from Harlan Nossan (Italy) by administering phenobarbital sodium (35 mg/dL) with drinking water for 3 d, followed by intraperitoneal injection of 100 μL/100 g body weight of CCl_4 in an equal volume of paraffin oil twice 1 wk for 6 wk. After the treatment with CCl_4, animals were administered with an intraperitoneal injection of 6E-CDCA, 10 mg/kg for 5 d while control animals were treated with vehicle alone (methyl-cellulose). At the end of the treatment, analysis of hepatic vascular responses to norepinephrine (from 10 nmol/L to 10 μmol/L) was performed using the isolated perfused rat liver preparation[26]. Briefly, a median laparotomy was performed and an PE-50 catheter was introduced into the inferior mesenteric vein and advanced to the portal vein for the measurement of portal pressure. The liver was perfused in a recirculating mode with Krebs solution equilibrated with CO_2, using a peristaltic pump as previously described[27]. The perfusion pressure was continuously monitored and recorded with a strain-gauge transducer connected to a PowerLab PC (A.D. Instruments, Milford, MA, USA). The preparation was allowed to stabilize for 20 min. The global viability of livers was assessed by standard criteria: gross appearance, stable pH of the perfusate, stable perfusion pressure for 20 min, and bile flow of > 1 μL/min per gram liver. The flow rate during each individual perfusion was maintained at a constant rate of 20 mL/min. Two additional groups of normal and cirrhosis rats were sacrificed and liver specimens were snap frozen in liquid nitrogen and stored at -70℃.

Serum biochemistry analysis

Serum bilirubin, aspartate aminotransferase (AST) and alanine aminotransferase (ALT) were measured by routine clinical chemistry testing performed on a Hitachi 717 automatic analyzer.

Liver histology

For histological examination, portions of the right and left liver lobes were fixed in 10% formalin, embedded in paraffin, sectioned, and stained with Sirius red.

Western blotting anti-smooth muscle actin (αSMA)

Total cellular proteins of frozen tissues were extracted using Tissue Protein Extraction reagent (Pierce) and solubilized in NuPage sample buffer (Invitrogen) containing Sample Reducing Agent (Invitrogen). Proteins were resolved by electrophoresis on 10% SDS-polyacrylamide gels and transferred to nitrocellulose membranes (Bio-Rad). After protein transfer, filters were probed with an αSMA primary antibody (Santa Cruz Biotechnology) for 1 h at room temperature. The anti-immunoglobulin G horseradish peroxidase conjugate (Bio-Rad) was used as the secondary antibody, and specific protein bands were visualized using Super Signal West Dura (Pierce), following the manufacturer's suggested protocol.

Statistics analysis

All values are expressed as mean ± SE of n observations per group. Comparisons of more than two groups were made with a one-way ANOVA with post-hoc Tukey's test. Comparison of two groups was made using Student's t test for unpaired data when appropriate. Differences were considered statistically significant if P was < 0.05.

RESULTS

CSE expression is regulated by FXR activation in vitro

We first investigated whether FXR activation modulates CSE gene expression. Serum-starved HepG2 cells, wild-type and stimulated with 10 μmol/L 6E-CDCA (a synthetic FXR ligand that activates FXR with an EC_{50} of about 300 nmol/L) were used in these experiments. As illustrated in Figure 1, FXR activation by this agent resulted in a robust induction of CSE expression
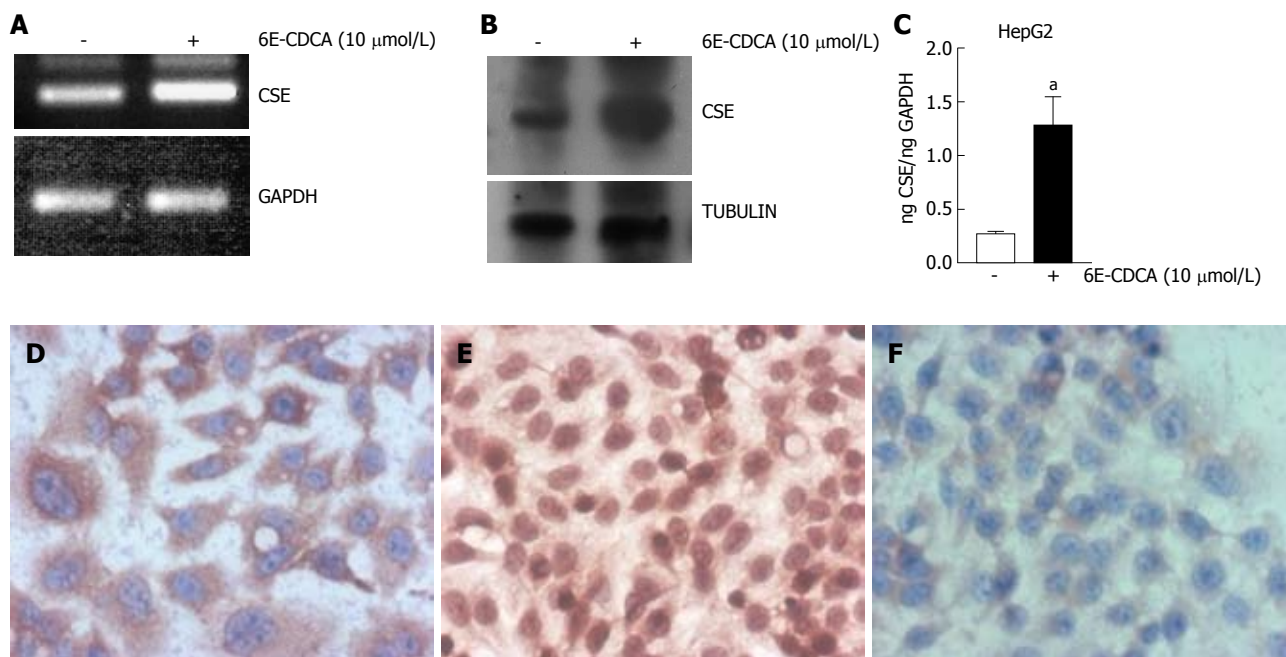
Figure 1 *CSE* gene expression is regulated by bile acids. A, B: Qualitative and quantitative PCR showing the up-regulation of CSE mRNA in HepG2 cell line stimulated with FXR ligand 6E-CDCA (10 μmol/L) for 18 h. Data are shown as mean ± SD of three experiments. [a]*P* < 0.05 *versus* not stimulated cells; C: Western blotting analysis showing the up-regulation of CSE protein in HepG2 cell line stimulated by 6E-CDCA 10 μmol/L for 18 h; D, E: Immunohistochemistry analysis of CSE expression in HepG2 cells non-treated (D) and treated (E) with 6E-CDCA (10 μmol/L) for 18 h (Magnification × 40); F: Negative control was obtained by cell staining only with the secondary antibody.

as measured by qualitative and quantitative PCR (Figure 1A and B; n = 3, P < 0.05 *vs* not stimulated cells) and Western blotting analysis (Figure 1C). Consistent with these findings, the immunohistochemical analysis of CSE expression demonstrated a significant increase in cell expression of this protein in HepG2 cells exposed to 10 μmol/L 6E-CDCA for 18 h (Figure 1E). These data establish that FXR activation in hepatocytes up-regulates CSE mRNA and protein expression.

Identification of an IR-1 sequence in the human CSE promoter

Having showed that the expression of human *CSE* gene is induced in response to FXR activation, we then investigated whether the CSE promoter contains any potential FXR binding sites. FXR binds preferentially to the IR1 element, and a putative IR1 sequence (CSE-IR1: AGTTCA*g*TGTACCT) was identified in the 5'-flanking region of the *CSE* gene (Figure 2A). This sequence is located 699 base pairs upstream of the transcriptional start site. To explore the functional role of this non-canonical IR1 sequence, four copies of the CSE-IR1 were cloned in the pGL3 basic vector [pGL3 (CSE-IR1)4x]. Additionally (Figure 2B), a construct containing a mutated IR1 site (CSE-IR1mutated: ATTTCT*g*TGTACCT) was generated and cloned in the pGL3 vector (pGL3CSE-IR1mutated). Using these reagents we investigated whether the identified FXR response element confers responsiveness to bile acid stimulation on the luciferase reporter gene. For this purpose, HepG2 cells co-transfected with pSG5-FXR and pSG5-RXR expression vectors were transiently transfected with the pGL3 (CSE-IR1)4x and then treated with natural FXR ligands: deoxycholic acid (DCA), litocholic acid (LCA), cholic acid (CA), chenodeoxycholic

acid (CDCA) and the synthetic FXR ligand 6E-CDCA at 25 μmol/L for 18 h. As show in Figure 2C, treating HepG2 cells with natural FXR ligands resulted in an approximately two to three-fold increase in luciferase activity, while the treatment with synthetic ligand resulted in an approximately eight-fold increase in luciferase activity (n = 3, P < 0.05 *vs* not treated cells). 6E-CDCA-mediated induction of reporter gene expression was concentration-dependent with an EC50 of 300 nmol/L (Figure 2D; n = 3, P < 0.05 *vs* not treated cells).

To further confirm the role of CSE-IR1 in mediating CSE induction in response to FXR activation, HepG2 cells co-transfected with pSG5-FXR and pSG5-RXR expression vectors were then transfected with pGL3 or pGL3 (CSE-IR1)4x or pGL3CSE-IR1mutated and then stimulated with 6E-CDCA 10 μmol/L for 18 h. Cells transfected with the pGL3 basic vector alone were used as an internal control (Figure 2E columns 1 and 2). As expected, co-transfection of pSG5-FXR and pSG5-RXR with pGL3 (CSE-IR1)4x resulted in a substantial increase in luciferase activity compared to co-transfection with the luciferase reporter vector alone. (Figure 2E, columns 1 and 3; n = 3, P < 0.05 *vs* not stimulated pGL3 transfected cells). The construct containing the wild-type IR-1 [pGL3 (CSE-IR1)4x] was found to cause about a four-fold increase in luciferase expression in the presence of a synthetic FXR ligand [Figure 2E, columns 3 and 4; n = 3, P < 0.05 *vs* not stimulated pGL3 (CSE-IR1)4x transfected cells]. The transactivation was abolished in cells transfected with a reporter gene in which the IR1 sequence was mutated [Figure 2E, column 5; n = 3, P < 0.05 *vs* not stimulated pGL3 (CSE-IR1)4x transfected cells] and the luciferase activity of the pGL3CSE-IR1mutated was similar to pGL3 basic. Similar results were obtained
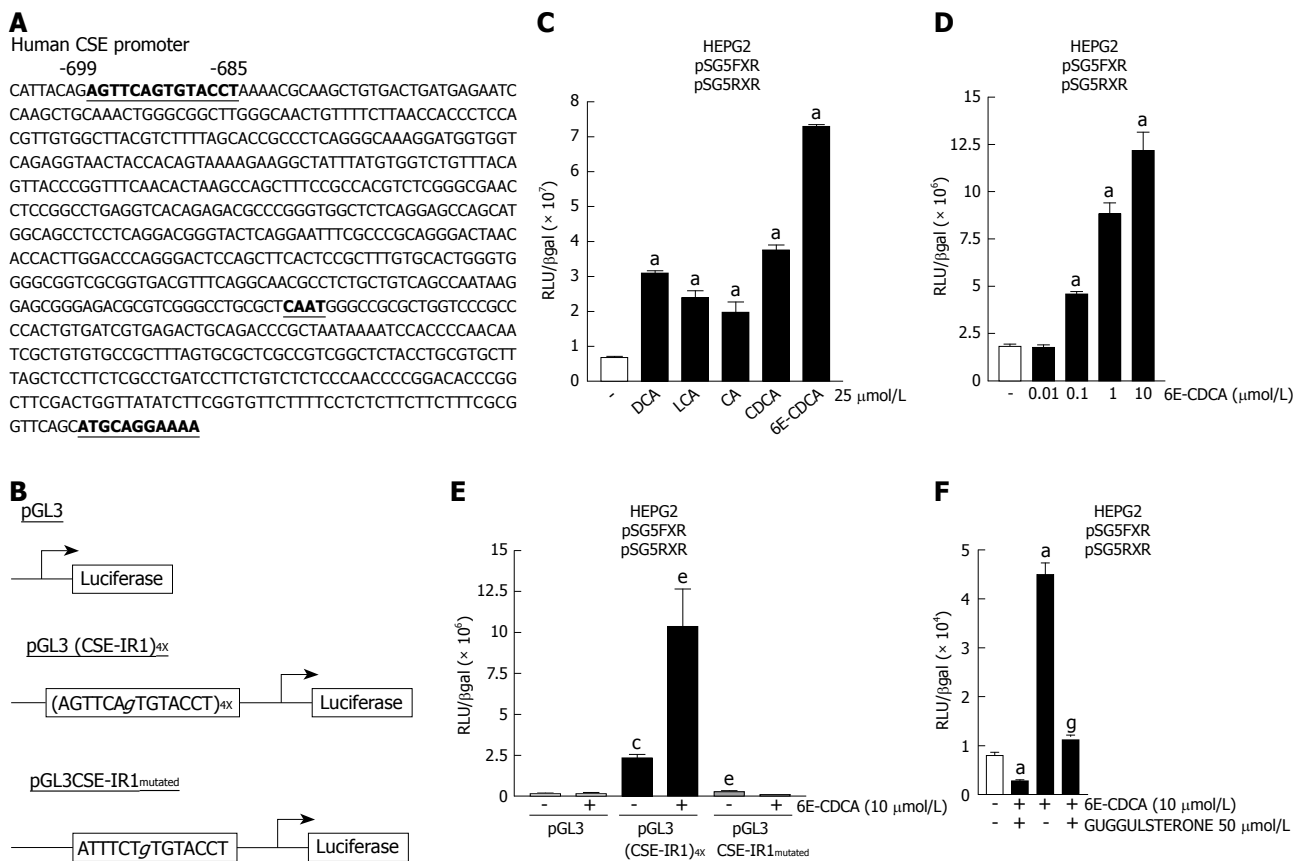
Figure 2 An FXR responsive element is expressed in the CSE promoter. A: Analysis of the promoter of the human *CSE* gene, showing a putative IR-1 site at -699/-685 base pairs upstream of the transcriptional start site ATG; B: Schematic representation of reporter constructs containing four CSE-IR1 elements [pGL3 (CSE-IR1)4x] or the mutated CSE-IR1 (pGL3CSE-IR1mutated); C: HepG2 cells were transfected with pSG5-FXR and pSG5-RXR expression vectors and with the construct containing four copies of the CSE-IR1 [pGL3 (CSE-IR1)4x]. Forty-eight hours after transfection, cells were stimulated with 25 μmol/L of DCA, LCA, CA, CDCA and 6E-CDCA for 18 h. Luciferase activity is shown as the ratio of luciferase to β-galactosidase activities. [a]$P < 0.05$ *versus* not treated cells; D: Dose-dependent induction of Luciferase activity by 6E-CDCA. [a]$P < 0.05$ *versus* not treated cells; E: Mutagenesis of CSE-IR1 results in a loss of activation by FXR ligands. HepG2 cells were transfected with pSG5-FXR and pSG5-RXR expression vectors and with pGL3 or pGL3 (CSE-IR1)4x or pGL3CSE-IR1mutated. Forty-eight hours after transfection, cells were stimulated with 10 μmol/L of 6E-CDCA for 18 h. Luciferase activity is show as the ratio of luciferase to β-galactosidase activities. [c]$P < 0.05$ *versus* not stimulated pGL3 transfected cells. [e]$P < 0.05$ *versus* not stimulated pGL3 (CSE-IR1)4x transfected cells; F: Guggulsterone abolished the transactivation of the CSE-IR1 element. HepG2 cells co-transfected with pSG5-FXR and pSG5-RXR expression vectors and with pGL3 (CSE-IR1)4x were stimulated with 50 μmol/L of guggulsterone alone or in combination with 10 μmol/L of 6E-CDCA. [a]$P < 0.05$ *versus* not treated cells. [g]$P < 0.05$ *versus* 6E-CDCA stimulated cells. Data represent the mean ± SD of three experiments.

using the FXR antagonist guggulsterone (Figure 2F). As expected, the stimulation of HepG2 cells co-transfected with pSG5-FXR, pSG5-RXR and pGL3 (CSE-IR1)4x with guggulsterone at 50 μmol/L for 18 h resulted in robust repression of luciferase activity with respect to non-stimulated cells (Figure 2F, columns 1 and 2; $n = 3$, $P < 0.05$ *vs* control cells). Treatment with 6E-CDCA resulted in about a four-fold increase of luciferase activity (Figure 2F, columns 1 and 3; $n = 3$, $P < 0.05$ *vs* not treated cells), while the transactivation was reduced in cells stimulated with both 6E-CDCA and guggulsterone with respect to cells stimulated only with 6E-CDCA (Figure 2F, columns 3 and 4; $n = 3$, $P < 0.05$ *vs* 6E-CDCA stimulated cells). These data establish that the IR1 motif in the proximal human CSE promoter is a functional FXR response element.

CSE-IR1 site binds FXR

To determine whether the IR1 element binds FXR, we performed an EMSA using the following biotin-labeled probes: CSE-IR1, CSE-IR1mutated and FXRE-IR1. CSE-IR1 biotin-labeled probe was incubated with nuclear extracts prepared from HepG2 cells left untreated or treated with 6E-CDCA 10 μmol/L for 18 h. As shown in Figure 3A, CSE-IR1 binding was detected in HEPG2 wild-type cells and exposure to 6E-CDCA enhanced this binding (Figure 3A, lanes 2 and 3). We confirmed the specificity of this interaction by adding 50-fold excess of unlabeled oligo or 1 μg anti FXR primary antibody or 1 μg anti RXR primary antibody (Figure 3A, lanes 4, 5 and 6). These approaches resulted in a reduction of DNA binding of the nuclear extract to CSE-IR1 probe. The specificity of the FXR interaction to CSE-IR1 was also confirmed using the mutated probe, CSE-IR1mutated, and the positive control, FXRE-IR1. DNA binding and supershift was completely abrogated using the CSE-IR1mutated probe, while the FXRE-IR1 probe caused same supershift as the CSE-IR1 probe (Figure 3A, lanes 7 and 8). To study the DNA-protein complex interaction within the context of chromatin, ChIP was performed using serum-starved HepG2 cells exposed to 6E-CDCA 10 μmol/L. As show in Figure 3B and C, qualitative and
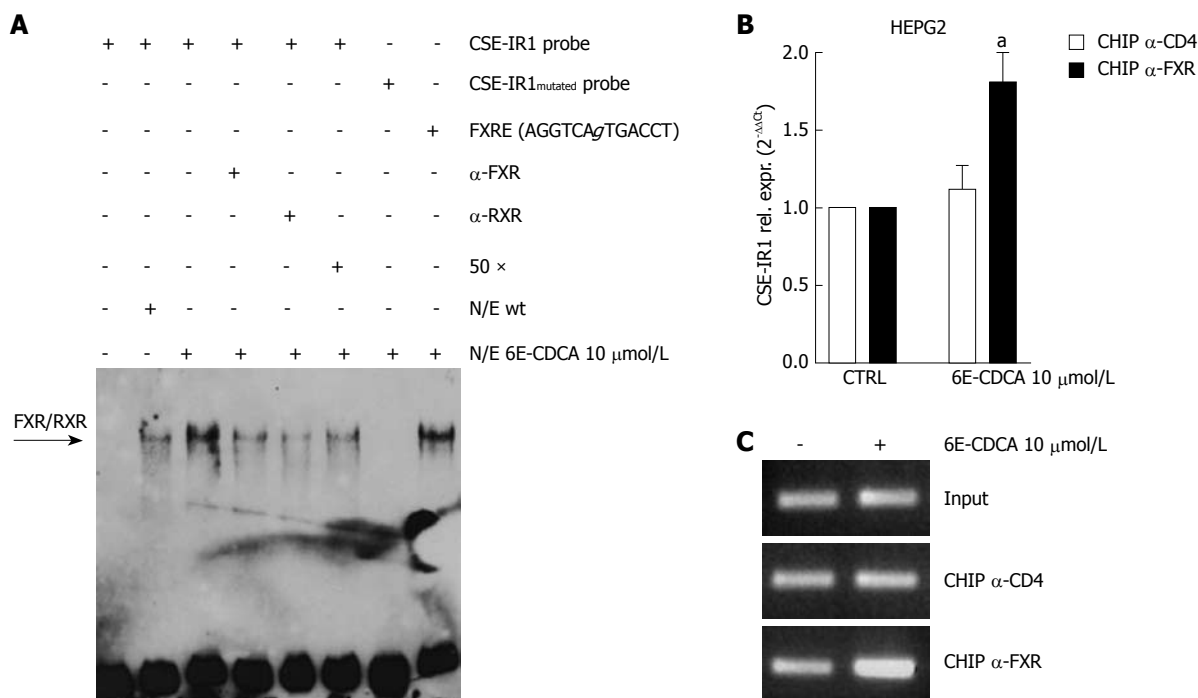
Figure 3 Activation of FXR regulates CSE expression. A: FXR/RXR bind to CSE-IR1 of the *CSE* gene. EMSAs were performed to analyze binding of FXR/RXR to the putative IR1 sequence in the CSE gene. CSE-IR1, CSE-IR1mutated and FXRE-IR1 probes, biotin-labeled, were used in this experiment. CSERE-IR1 probe was incubated with nuclear extracts from HepG2 cells not treated or treated with 6E-CDCA 10 μmol/L for 18 h. Competition experiments were performed using a 50-fold excess of unlabeled oligo or 1 μg of FXR antibody or 1 μg of RXR antibody. CSE-IR1mutated and FXRE-IR1 probes were incubated with nuclear extracts from HepG2 stimulated cells; B: CSE-IR1 site binds FXR in the context of intact chromatin structures. ChIP experiments were performed with HepG2 cells. Chromatin was prepared and immunoprecipitated with antibodies directed against FXR and CD4. CD4 antibody was used as a negative control. Real-time PCR of the immunoprecipitated DNA by using the primer pairs indicated in Table 1. Data represent the mean ± SD of three experiments. [a]$P < 0.05$ *versus* not treated cells; C: Qualitative PCR of the immunoprecipitated DNA by using the primer pairs indicated in Table 1.
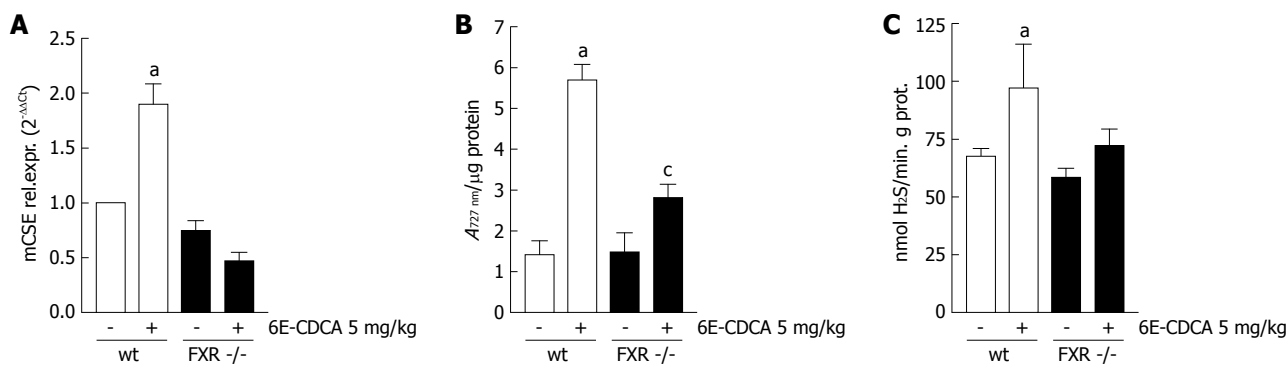

Figure 4 CSE expression/activity is regulated with an FXR ligand *in vivo*. A: FXR +/+ and FXR -/- mice were treated for 3 d with vehicle or with 6E-CDCA 5 mg/kg body weight. Total RNA from liver of FXR +/+ and FXR -/- mice was subjected to real-time PCR quantification of *CSE* gene expression. [a]$P < 0.05$ *versus* FXR +/+ control mice; B: FXR +/+ and FXR -/- mice were treated for three days with vehicle or with 6E-CDCA 5 mg/kg body weight. Livers from FXR +/+ and FXR -/- mice were homogenized in cold PBS to evaluate CSE activity. [a]$P < 0.05$ *versus* FXR +/+ control mice. [c]$P < 0.05$ *versus* FXR -/- control mice; C: FXR +/+ and FXR -/- mice were treated for 3 d with vehicle or with 6E-CDCA 5 mg/kg body weight. Livers from FXR +/+ and FXR -/- mice were homogenized in cold PBS to evaluate H2S production. [a]$P < 0.05$ *versus* FXR +/+ control mice. Data represent the mean ± SD of six experiments.

quantitative PCR performed with primers flanking the CSE promoter containing the IR1 sequence, confirmed the binding of FXR at the *CSE* gene (Figure 3B; *n* = 3, *P* < 0.05 *vs* not treated cells). Thus, the functionality of this IR1 site was further confirmed in the context of intact chromatin structures.

CSE expression is induced by 6E-CDCA *in vivo*
To investigate whether FXR regulates *CSE* gene expression *in vivo*, wild-type and FXR -/- mice were

administered with 6E-CDCA 10 mg/kg for 3 d and sacrificed to measure liver CSE expression, CSE activity and H2S production. As show in Figure 4A, while an induction of CSE mRNA expression was seen in wild-type mice treated with 6E-CDCA (*n* = 6, *P* < 0.05 *vs* FXR +/+ control mice), this effect was not observed in FXR -/- mice, confirming that the *CSE* gene is a specific target of FXR. Interestingly, FXR activation by 6E-CDCA increased CSE activity in both wild-type and FXR -/- mice (Figure 4B; *n* = 6, *P* < 0.05 *vs* FXR +/+
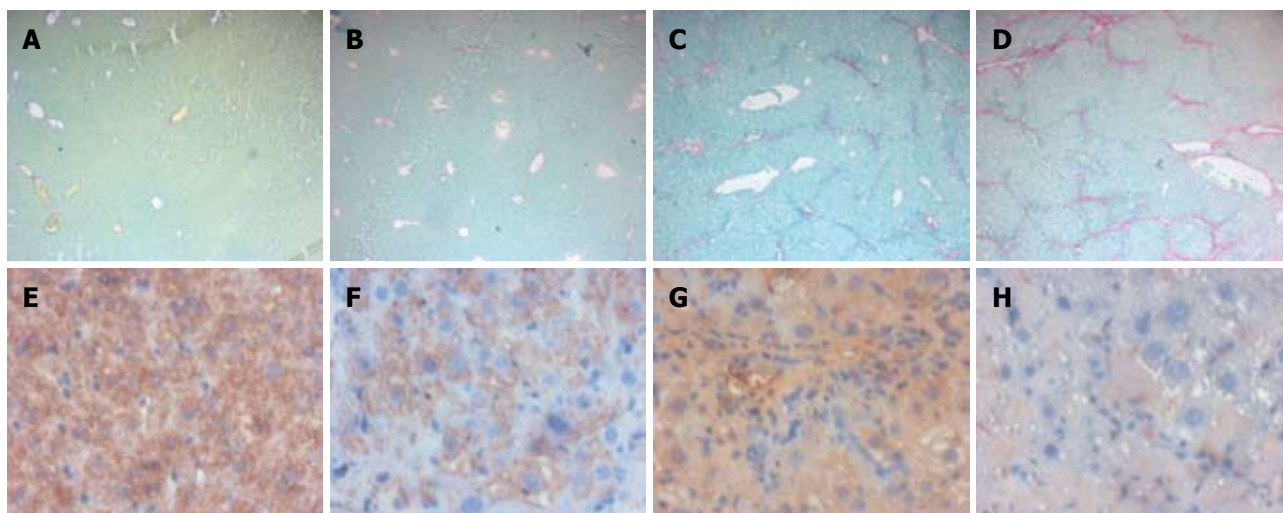
Figure 5 FXR loss of function sensitizes mice to CCl4-induced liver fibrosis. A: Sirius red staining of liver section obtained from FXR +/+ mice; B: Sirius red staining of liver section obtained from FXR -/- mice; C: Sirius red staining of liver section obtained from FXR +/+ mice treated with CCl4; D: Sirius red staining of liver section obtained from FXR -/- mice treated with CCl4; E: Liver section stained with CSE monoclonal antibody obtained from FXR +/+ mice; F: Liver section stained with CSE monoclonal antibody obtained from FXR -/- mice; G: Liver section stained with CSE monoclonal antibody obtained from FXR +/+ mice treated with CCl4; H: Liver section stained with CSE monoclonal antibody obtained from FXR -/- mice treated with CCl4.

Table 2 Effect of loss of FXR on liver injury induced by 12 administrations of CCl4 (6 wk)			
	AST (U/L)	ALT (U/L)	Bilirubin (mg/dL)
FXR +/+ naive	127 ± 15	48 ± 8	0.015 ± 0.001
FXR +/+ CCl4	250 ± 40[a]	369 ± 35[a]	0.118 ± 0.004[a]
FXR -/- naive	143 ± 10	79 ± 25[a]	0.068 ± 0.004[a]
FXR -/- CCl4	740 ± 230[c,e]	354 ± 137[c]	0.252 ± 0.02[c,e]

Data are mean ± SD of six mice. [a]$P < 0.05$ vs FXR +/+ control mice; [c]$P < 0.05$ vs FXR -/- control mice; [e]$P < 0.05$ vs CCl4 FXR +/+ mice.

control mice, $P < 0.05$ vs FXR -/- control mice). Taken together, these data suggest that while mRNA expression of CSE is regulated by an FXR-dependent mechanism, the induction of CSE activity by bile acids might be regulated by an FXR independent mechanism, possibly by TGR5 activation induced by bile acids. Finally, liver H2S generation was significantly up-regulated by 6E-CDCA treatment in FXR +/+ mice but not in FXR -/- mice (Figure 4C; $n = 6$, $P < 0.05$ vs FXR +/+ control mice).

FXR loss of function sensitizes mice to CCl4-induced liver fibrosis

We next investigated whether in vivo loss of FXR function sensitizes mice to development of liver fibrosis induced by administration of CCl4. AST, ALT and bilirubin are commonly used biochemical markers of liver damage. As show in Table 2, the levels of ALT and bilirubin, but not of AST, in FXR -/- mice were much higher compared with the wild-type mice. In vivo administration of CCl4 showed a significant increase of AST, ALT and bilirubin in FXR -/- mice with respect to FXR +/+ control mice (Table 2). Morphometric analysis of FXR +/+ and FXR -/- liver sections stained with Sirius red showed a normal distribution of collagen, with a variable amount in the portal tract and a thin rim around the terminal hepatic vein (Figure 5A and B), while histological evaluation of liver specimens obtained from FXR -/- mice treated

with CCl4 for 6 wk showed extensive perilobular fibrosis, resulting in an increase in the surface area of hepatic collagen in comparison with control FXR +/+ mice treated with CCl4 (Figure 5C and D). Expression of CSE, observed by histochemical staining of liver sections, was reduced in FXR -/- mice compared with the wild-type mice (Figure 5E and F). Furthermore, FXR -/- mice administered with CCl4 showed a significant reduction in CSE expression compared to FXR +/+ mice treated with CCl4 (Figure 5G and H). Taken together, these data confirmed that mice lacking FXR are more likely to develop liver fibrosis, and that FXR loss of function correlates with reduction of CSE protein expression in the liver.

FXR activation restores H2S production and CSE activity in a rodent model of liver cirrhosis

We then investigated whether in vivo administration of FXR ligands modulate CSE expression, the activity of the enzyme and H2S production, in wild-type but not in FXR -/- mice administered with CCl4. As show in Figure 6A, development of liver injury is associated with a significant reduction in CSE mRNA expression, in both the wild-type and FXR -/- mice treated with CCl4 for 6 wk. In wild-type mice, administration of an FXR ligand resulted in a robust induction of CSE expression. This effect was not reproduced in FXR -/- mice, confirming the specificity of 6E-CDCA (Figure 6A; $n = 6$, $P < 0.05$ vs FXR +/+ control mice. $P < 0.05$ vs CCl4 FXR +/+ mice). Similarly, we found that α1-collagen mRNA expression was down-regulated by 6E-CDCA in wild-type mice but not in FXR -/- mice (Figure 6B; $n = 6$, $P < 0.05$ vs FXR +/+ control mice. $P < 0.05$ vs CCl4 FXR +/+ mice. $P < 0.05$ vs FXR -/- control mice). In addition, we found that liver CSE activity was down-regulated by CCl4 administration in both FXR +/+ and FXR -/- mice, but this effect was reversed by treating the mice with 6E-CDCA (Figure 6C; $n = 6$, $P < 0.05$ vs FXR +/+ control mice. $P < 0.05$ vs CCl4 FXR +/+ mice.
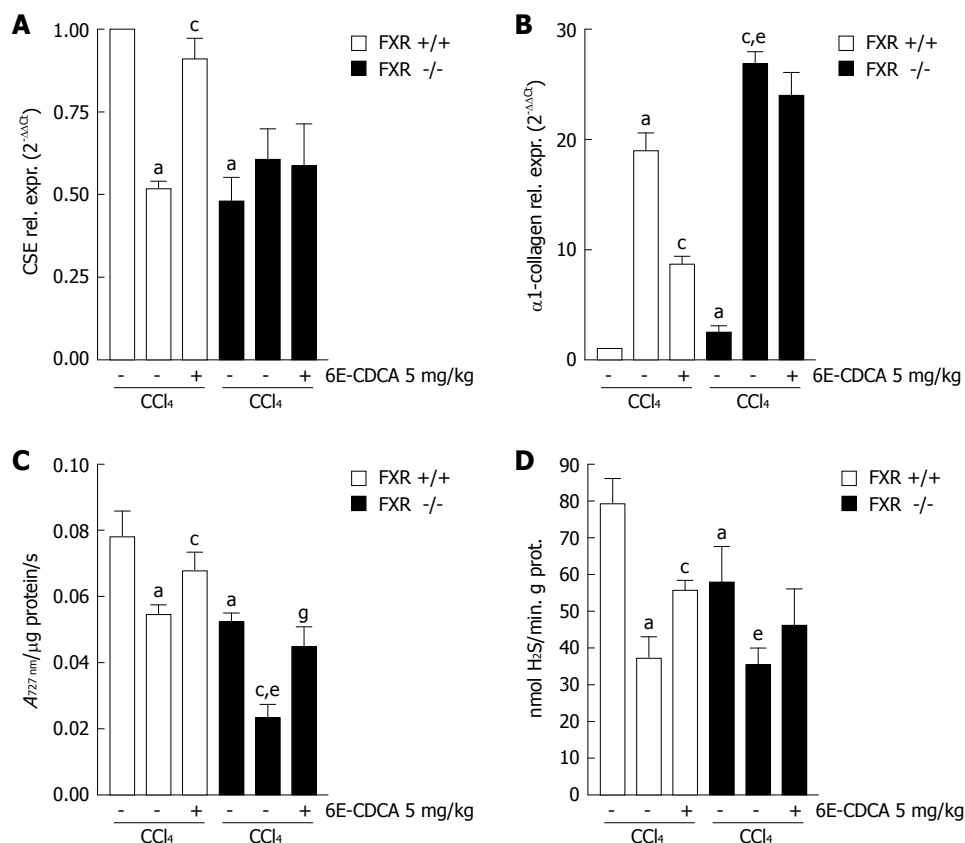
Figure 6 FXR activation induces *CSE* gene expression and regulated CSE activity in the liver with cirrhosis. FXR +/+ and FXR -/- mice were treated with CCl4 and 6E-CDCA as described in the methods section. A and B: Quantitative real-time PCR of CSE mRNA and α1-collagen mRNA from FXR +/+ and FXR -/- liver homogenates; C: Liver CSE activity; D: Liver H2S production. Data are mean ± SD of six mice. [a]$P < 0.05$ *versus* FXR+/+ control mice. [c]$P < 0.05$ *versus* CCl4 FXR +/+ mice. [e]$P < 0.05$ *versus* FXR -/- control mice. [g]$P < 0.05$ *versus* CCl4 FXR -/- mice.

$P < 0.05$ *vs* FXR -/- control mice. $P < 0.05$ *vs* CCl4 FXR -/- mice). CCl4 administration down-regulated liver H2S production in both FXR +/+ and FXR -/- mice, while the administration of 6E-CDCA enhanced liver H2S generation only in FXR +/+ mice (Figure 5D; $n = 6$, $P < 0.05$ *vs* FXR +/+ control mice. $P < 0.05$ *vs* CCl4 FXR +/+ mice. $P < 0.05$ *vs* FXR -/- control mice).

FXR activation reduces portal perfusion pressure response to norepinephrine in cirrhotic rat liver

The reduction of CSE expression in the cirrhotic liver contributes to the development of increased intrahepatic resistance and portal hypertension. We therefore investigated whether *in vivo* administration of an FXR ligand modulates hepatic resistance in cirrhotic rats. As shown in Figure 7, the development of liver injury in rats reduced the expression of FXR and CSE (Figure 7A and B; $n = 6$, $P < 0.05$ *vs* control rats, $P < 0.05$ *vs* CCl4 rats) while small heterodimer partner mRNA expression was unaffected (Figure 7C; $n = 6$, $P < 0.05$ *vs* CCl4 rats). In contrast, CCl4 administration up-regulated α1-collagen and αSMA mRNA (Figure 7D and E; $n = 6$, $P < 0.05$ *versus* control rats) Thus, treating CCl4 rats with 6E-CDCA resulted in a robust induction of *FXR*, *SHP* and *CSE* genes (Figure 7A-C; $n = 6$, $P < 0.05$ *vs* CCl4 rats), as well as suppression of α1-collagen gene expression (Figure 7D; $n = 6$, $P < 0.05$ *vs* CCl4 rats). The CSE activity was strongly down-regulated by administration of CCl4 in rats and the treatment with 6E-CDCA led to an increase of this enzyme activity (Figure 7F; $n = 6$, $P < 0.05$ *versus* control rats; $P < 0.05$ *vs* CCl4 rats). Furthermore, as shown in Figure 8, the expression of CSE and αSMA was also investigated at the protein level by Western

blotting analysis. We found that the CSE protein was strongly down-regulated during liver injury and that 6E-CDCA treatment resulted in a robust induction of this enzyme (Figure 8A). In contrast, CCl4 treatment up-regulated the pro-fibrogenetic marker αSMA and administration of 6E-CDCA resulted in a suppression of this protein (Figure 8B). We then investigated whether FXR activation by a synthetic ligand lowers portal pressure in rodent models of liver injury. Under basal conditions, portal pressure was significantly higher in cirrhotic rats compared with the control rats (Figure 9A; $n = 6$, $P < 0.05$ *vs* control rats). In the cirrhotic rats, treatment with 6E-CDCA significantly decreased the portal pressure (Figure 9A; $n = 6$, $P < 0.05$ *vs* CCl4 rats). Finally, data shown in Figure 9B demonstrated that in livers with cirrhosis, norepinephrine produced a dose-dependent increase in the portal perfusion pressure compared with control rats (Figure 9B; $n = 6$, $P < 0.05$ *vs* control rats). In contrast, treatment with 6E-CDCA reduced the hyper-responsiveness of livers with cirrhosis to norepinephrine (Figure 9B; $n = 6$, $P < 0.05$ *versus* CCl4 rats).

DISCUSSION

Portal hypertension is associated with changes in intrahepatic, systemic, and portosystemic collateral circulation[28,29]. Alterations in vasoreactivity (vasodilatation and vasoconstriction) play a central role in the pathogenesis of this condition by contributing to increased intrahepatic resistance, hyperdynamic circulation and expansion of the collateral circulation[28,29]. The molecular basis of the vascular abnormalities that contribute to development of
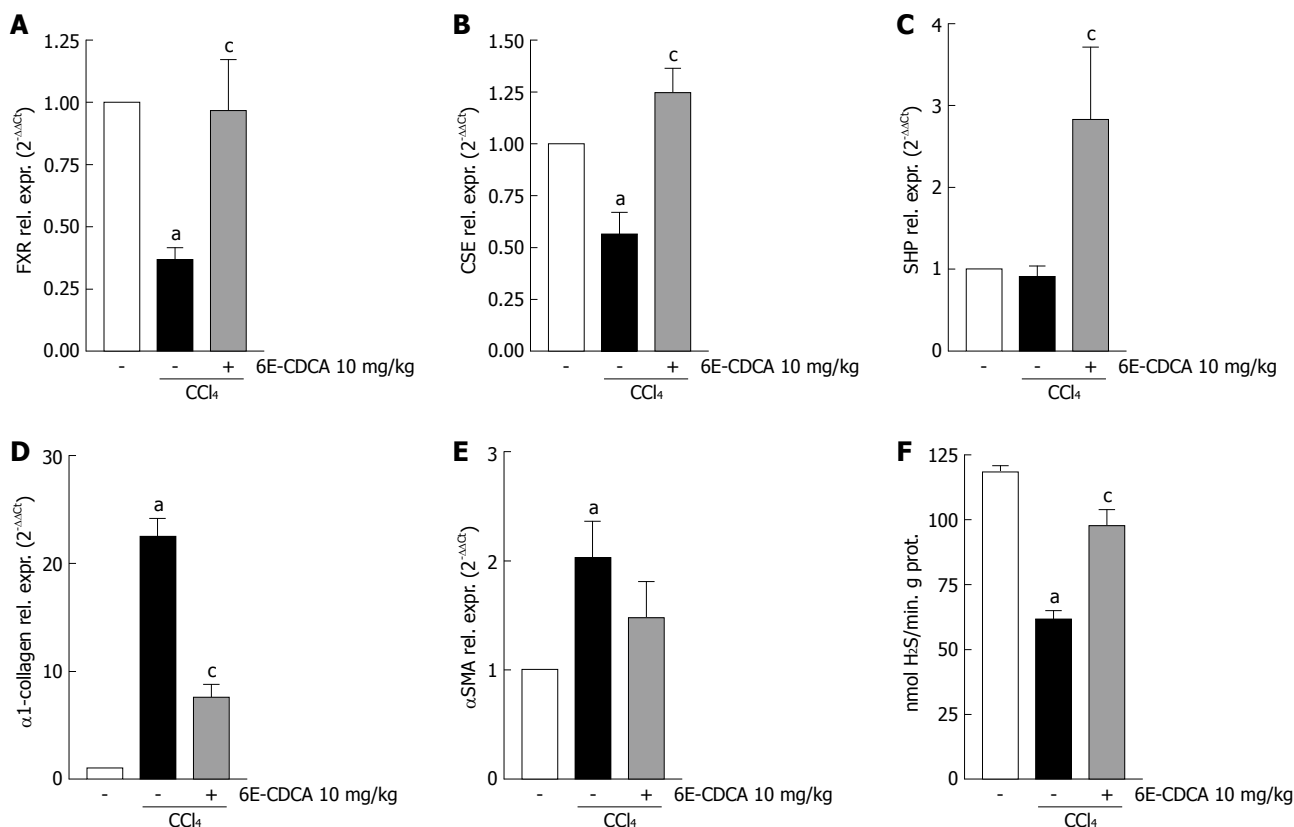
Figure 7 FXR activation induces both CSE mRNA expression and activity in rats with liver cirrhosis. Quantitative real-time PCR of (A) FXR mRNA, (B) CSE mRNA, (C) SHP mRNA, (D) α1-collagen mRNA, (E) αSMA mRNA from rats liver homogenates and (F) Rat liver CSE activity. Data are mean ± SD of six mice. [a]$P < 0.05$ versus control rats. [c]$P < 0.05$ versus CCl4 rats.
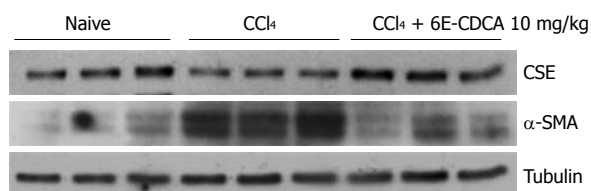

Figure 8 FXR activation induces CSE protein expression and reduces αSMA protein level in rat's liver with cirrhosis. Western blotting analysis of CSE, αSMA and tubulin on liver homogenates. From left to right: Lanes 1-3, liver samples from control rats; Lanes 4-6, liver samples from rats administered CCl4; Lanes 7-9, liver samples from rats administered CCl4 and 10 mg/kg 6E-CDCA.

portal hypertension are only partially identified[17,30-32]. A diminution in endothelial-nitric-oxide-synthase-derived NO production by liver sinusoidal cells contributes to this process by impairing the ability of hepatic microcirculation to vasodilate and therefore increases intrahepatic resistance[33]. We have previously described that along with NO, H2S causes a direct relaxation of intrahepatic microcirculation, suggesting a physiological role for this gaseous mediator in regulating resistance of intrahepatic microcirculation. H2S exerts a portal-pressure-lowering effect in normal rats as well as in rats rendered cirrhotic by CCl4 administration, an experimental setting characterized by endothelial dysfunction of intrahepatic circulation and reduced generation of NO[9]. Finally, we have previously provided evidence that a robust reduction of H2S generation takes place in cirrhotic rats and that this defect is linked to a decrease in the liver expression

and activity of CSE, a key enzyme in the pathway that leads to generation of H2S[17].

Little is known about the molecular mechanism responsible for the regulation of *CSE* gene expression and there is no evidence of the regulation of the *CSE* gene by nuclear receptors. FXR is one of the major nuclear receptors responsible for regulation of liver metabolism, therefore, we decided to study whether CSE expression in the liver was regulated by FXR. In the current study, we have shown, for the first time, that the liver expression of CSE is regulated by bile acids by means of an FXR mediated mechanism. By Western blotting, qualitative and quantitative PCR, as well as immunohistochemical analysis, we have shown that expression of CSE (mRNA and protein) in HepG2 cells is induced by treatment with bile acids and 6E-CDCA, a semi-synthetic FXR ligand. The molecular mechanism of the CSE activation by FXR was revealed by identifying a sequence in the 5' flanking region of the *CSE* gene, containing an element composed of two inverted repeats separated by one nucleotide (a potential IR1 binding site). Four copies of this IR1 binding site were cloned into the pGL3 vector containing the luciferase reporter gene, and in addition, a single copy of the IR1 binding site was mutated and cloned in the pGL3 vector. Co-transfection of HepG2 cells with FXR and RXR resulted in transactivation of the CSE promoter in the presence of an FXR ligand, while the mutation of the IR1 binding site and the treatment with an FXR antagonist, such as guggulsterone, abrogated this response. The FXR/RXR heterodimer bound specifically
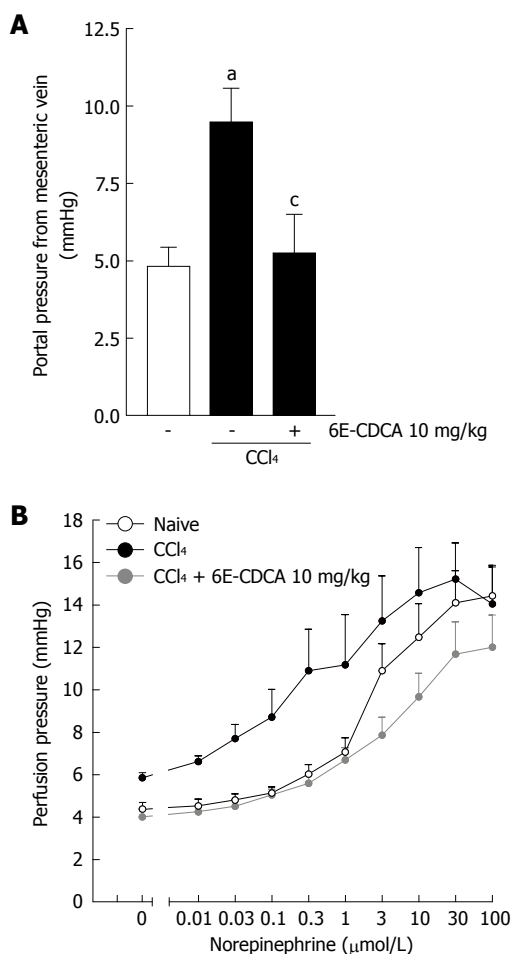
A

B

Figure 9 FXR activation reduces portal pressure in rat liver with cirrhosis. Data are mean ± SD of six mice. A: Basal portal pressure from mesenteric vein. [a]$P < 0.05$ *versus* control rats. [c]$P < 0.05$ *versus* CCl4 rats; B: Effects of 6E-CDCA on pre-contracted rat liver with cirrhosis. [a]$P < 0.05$ *versus* control rats. [c]$P < 0.05$ *versus* CCl4 rats.

to the CSE IR1 binding site, but not to the mutant form, as shown by a gel mobility shift assay using nuclear extracts from HepG2 cells not treated or treated with 6E-CDCA. The functionality of this IR1 site was also confirmed in the context of intact chromatin structures by a ChIP assay.

The role of FXR in the regulation of CSE has been further investigated *in vivo*, in mice harboring a targeted disruption of the *FXR* gene. These mice lack functional FXR and are unable to correctly regulate bile acids biosynthesis and excretion. Interestingly, when compared to the wild-type, FXR -/- mice displayed significantly lower levels of CSE and a reduced ability to produce H2S. Similarly to the *in vitro* results, we found that in the normal liver, CSE expression was significantly increased when mice were fed a chow diet supplemented with 5 mg/kg body weight of 6E-CDCA, while the FXR ligand failed to up-regulate CSE mRNA expression in FXR knock-out mice. In contrast, administration of 6E-CDCA induced CSE activity in both wild-type and FXR knock-out mice. This finding suggested that the activity of the enzyme might be regulated by bile acids at the post-translational level, and a possible mechanism could be linked to the activation of the TGR5 induced phosphorylation cascade through the bile acids. We also confirmed that CSE liver

expression was down-regulated in an animal model of liver damage induced by CCl4 and that the reduction of H2S generation seen in this model is likely to contribute to portal hypertension. One of the major findings of this study was the demonstration that mice lacking FXR are more likely to develop liver fibrosis and that loss of FXR function correlates with reduction of CSE protein expression in the liver. Treatment with an FXR ligand increased both CSE expression and activity in the cirrhotic liver, restoring the ability of injured livers to generate H2S. These findings were not observed in cirrhotic FXR -/- mice treated with 6E-CDCA.

In addition to inhibition of NO formation by sinusoidal endothelial cells, homocysteine triggers an H2S-sensitive contraction of hepatic stellate cells *in vitro*[18]. Contraction of presinusoidal myofibroblasts has relevance in regulating intrahepatic resistance and short-term administration of 6E-CDCA regulates CSE expression in normal mice, therefore, we investigated whether acute administration of an FXR ligand effectively modulates CSE expression in CCl4 treated rats and whether this treatment was effective in correcting hepatic microcirculation hyper-responsiveness to norepinephrine. Despite the fact that even 3 d of administration of 6E-CDCA attenuated expression of 1-collagen and SMA mRNA, this anti-fibrotic activity did not completely explain the rapid re-induction of CSE expression in the liver that was associates with a restored ability to generate H2S and a robust attenuation of hyper-responsiveness of cirrhotic livers to norepinephrine. The ability of the FXR ligand to lower portal pressure and to correct the enhanced vasomotor activity is consistent with the finding that perfusion of cirrhotic livers with H2S attenuates the endothelial dysfunction that takes place in injured livers.

In conclusion, we have shown that CSE, a key enzyme in the trans-sulfuration pathway, is an FXR-regulated gene. Despite the fact that the level of expression/function of FXR in chronic liver disorders is still unknown, FXR is severely down-regulated in several models of liver injury. Reduction of FXR-regulated genes might contribute to the metabolic dysfunction that takes place in advanced cirrhosis. By linking the deficiency of CSE to the FXR activity the present study provides a new molecular explanation of the pathophysiology of portal hypertension. It also proposes the concept that FXR agonists might correct for the altered generation of endogenous hepatic vasodilators that takes place in chronic liver diseases.

COMMENTS

Background

Portal hypertension is primarily caused by the increase in resistance to portal outflow and an increase in splanchnic blood flow. Alterations in systemic and liver vasoreactivity play a central role in the pathogenesis of this condition by contributing to increased intrahepatic resistance, hyperdynamic circulation and expansion of the collateral circulation. Nitric oxide and hydrogen sulfide (H2S) cause a direct relaxation of intrahepatic microcirculation suggesting a physiological role for these gaseous mediators in regulating resistance of intrahepatic microcirculation.

Research frontiers

Understanding of the pathophysiology of portal hypertension is essential in the development of new pharmacological treatment of this condition.

Innovations and breakthroughs

Farnesoid X receptor (FXR) is a bile acid sensor and upon activation it reduces the conversion of cholesterol into bile acids and increases bile acid excretion from hepatocytes by activating canalicular transporters. The authors demonstrate that cystathionase, a key enzyme for H_2S production, is an FXR regulated gene.

Applications

FXR agonists might correct for the altered generation of endogenous hepatic vasodilators that takes place in chronic liver diseases.

Peer review

The manuscript by Renga et al is a comprehensive study demonstrating the effect of FXR activation by bile acids on the expression of cystathione-γ-lyase and subsequent hydrogen disulfide production. Furthermore, mice lacking the FXR are more susceptible to the liver damage induced by CCl_4. This is a thorough and well-written manuscript that highlights important bile acid signaling events.

REFERENCES

1   **Ishii I**, Akahoshi N, Yu XN, Kobayashi Y, Namekata K, Komaki G, Kimura H. Murine cystathionine gamma-lyase: complete cDNA and genomic sequences, promoter activity, tissue distribution and developmental expression. *Biochem J* 2004; **381**: 113-123

2   **Yamanishi T**, Tuboi S. The mechanism of the L-cystine cleavage reaction catalyzed by rat liver gamma-cystathionase. *J Biochem* 1981; **89**: 1913-1921

3   **Stipanuk MH**. Sulfur amino acid metabolism: pathways for production and removal of homocysteine and cysteine. *Annu Rev Nutr* 2004; **24**: 539-577

4   **Kim SK**, Choi KH, Kim YC. Effect of acute betaine administration on hepatic metabolism of S-amino acids in rats and mice. *Biochem Pharmacol* 2003; **65**: 1565-1574

5   **Rao AM**, Drake MR, Stipanuk MH. Role of the transsulfuration pathway and of gamma-cystathionase activity in the formation of cysteine and sulfate from methionine in rat hepatocytes. *J Nutr* 1990; **120**: 837-845

6   **Triguero A**, Barber T, García C, Puertes IR, Sastre J, Viña JR. Liver intracellular L-cysteine concentration is maintained after inhibition of the trans-sulfuration pathway by propargylglycine in rats. *Br J Nutr* 1997; **78**: 823-831

7   **Stipanuk MH**, Dominy JE Jr, Lee JI, Coloso RM. Mammalian cysteine metabolism: new insights into regulation of cysteine metabolism. *J Nutr* 2006; **136**: 1652S-1659S

8   **Drake MR**, De La Rosa J, Stipanuk MH. Metabolism of cysteine in rat hepatocytes. Evidence for cysteinesulphinate-independent pathways. *Biochem J* 1987; **244**: 279-286

9   **Hosoki R**, Matsuki N, Kimura H. The possible role of hydrogen sulfide as an endogenous smooth muscle relaxant in synergy with nitric oxide. *Biochem Biophys Res Commun* 1997; **237**: 527-531

10 **Teague B**, Asiedu S, Moore PK. The smooth muscle relaxant effect of hydrogen sulphide in vitro: evidence for a physiological role to control intestinal contractility. *Br J Pharmacol* 2002; **137**: 139-145

11 **Cheng Y**, Ndisang JF, Tang G, Cao K, Wang R. Hydrogen sulfide-induced relaxation of resistance mesenteric artery beds of rats. *Am J Physiol Heart Circ Physiol* 2004; **287**: H2316-H2323

12 **Zhao W**, Zhang J, Lu Y, Wang R. The vasorelaxant effect of H(2)S as a novel endogenous gaseous K(ATP) channel opener. *EMBO J* 2001; **20**: 6008-6016

13 **Fiorucci S**, Antonelli E, Distrutti E, Rizzo G, Mencarelli A, Orlandi S, Zanardo R, Renga B, Di Sante M, Morelli A, Cirino G, Wallace JL. Inhibition of hydrogen sulfide generation contributes to gastric injury caused by anti-inflammatory nonsteroidal drugs. *Gastroenterology* 2005; **129**: 1210-1224

14 **Zhong G**, Chen F, Cheng Y, Tang C, Du J. The role of hydrogen sulfide generation in the pathogenesis of hypertension in rats induced by inhibition of nitric oxide synthase. *J Hypertens* 2003; **21**: 1879-1885

15 **Bellentani S**, Pecorari M, Cordoma P, Marchegiano P, Manenti F, Bosisio E, De Fabiani E, Galli G. Taurine increases bile acid pool size and reduces bile saturation index in the hamster. *J Lipid Res* 1987; **28**: 1021-1027

16 **Murakami S**, Kondo Y, Toda Y, Kitajima H, Kameo K, Sakono M, Fukuda N. Effect of taurine on cholesterol metabolism in hamsters: up-regulation of low density lipoprotein (LDL) receptor by taurine. *Life Sci* 2002; **70**: 2355-2366

17 **Fiorucci S**, Antonelli E, Mencarelli A, Orlandi S, Renga B, Rizzo G, Distrutti E, Shah V, Morelli A. The third gas: H2S regulates perfusion pressure in both the isolated and perfused normal rat liver and in cirrhosis. *Hepatology* 2005; **42**: 539-548

18 **Distrutti E**, Mencarelli A, Santucci L, Renga B, Orlandi S, Donini A, Shah V, Fiorucci S. The methionine connection: homocysteine and hydrogen sulfide exert opposite effects on hepatic microcirculation in rats. *Hepatology* 2008; **47**: 659-667

19 **Forman BM**, Goode E, Chen J, Oro AE, Bradley DJ, Perlmann T, Noonan DJ, Burka LT, McMorris T, Lamph WW, Evans RM, Weinberger C. Identification of a nuclear receptor that is activated by farnesol metabolites. *Cell* 1995; **81**: 687-693

20 **Seol W**, Choi HS, Moore DD. Isolation of proteins that interact specifically with the retinoid X receptor: two novel orphan receptors. *Mol Endocrinol* 1995; **9**: 72-85

21 **Pellicciari R**, Costantino G, Fiorucci S. Farnesoid X receptor: from structure to potential clinical applications. *J Med Chem* 2005; **48**: 5383-5403

22 **Edwards PA**, Kast HR, Anisfeld AM. BAREing it all: the adoption of LXR and FXR and their roles in lipid homeostasis. *J Lipid Res* 2002; **43**: 2-12

23 **Nishi N**, Tanabe H, Oya H, Urushihara M, Miyanaka H, Wada F. Identification of probasin-related antigen as cystathionine gamma-lyase by molecular cloning. *J Biol Chem* 1994; **269**: 1015-1019

24 **Ogasawara Y**, Ishii K, Tanabe S. Enzymatic assay of gamma-cystathionase activity using pyruvate oxidase-peroxidase sequential reaction. *J Biochem Biophys Methods* 2002; **51**: 139-150

25 **Sinal CJ**, Tohkin M, Miyata M, Ward JM, Lambert G, Gonzalez FJ. Targeted disruption of the nuclear receptor FXR/BAR impairs bile acid and lipid homeostasis. *Cell* 2000; **102**: 731-744

26 **Fiorucci S**, Antonelli E, Morelli O, Mencarelli A, Casini A, Mello T, Palazzetti B, Tallet D, del Soldato P, Morelli A. NCX-1000, a NO-releasing derivative of ursodeoxycholic acid, selectively delivers NO to the liver and protects against development of portal hypertension. *Proc Natl Acad Sci USA* 2001; **98**: 8897-8902

27 **Grossman HJ**, Grossman VL, Bhathal PS. Hemodynamic characteristics of the intrahepatic portal vascular bed over an extended flow range: a study in the isolated perfused rat liver. *Hepatology* 1995; **21**: 162-168

28 **Shah V**. Cellular and molecular basis of portal hypertension. *Clin Liver Dis* 2001; **5**: 629-644

29 **Shah V**. Molecular mechanisms of increased intrahepatic resistance in portal hypertension. *J Clin Gastroenterol* 2007; **41** Suppl 3: S259-S261

30 **Bosch J**, Pizcueta P, Feu F, Fernàndez M, Garcìa-Pagan JC. Pathophysiology of portal hypertension. *Gastroenterol Clin North Am* 1992; **21**: 1-14

31 **Gonzàlez-Abraldes J**, Garcìa-Pagan JC, Bosch J. Nitric oxide and portal hypertension. *Metab Brain Dis* 2002; **17**: 311-324

32 **Moreau R**, Lebrec D. Molecular and structural basis of portal hypertension. *Clin Liver Dis* 2006; **10**: 445-457, vii

33 **Bosch J**, Garcìa-Pagan JC. Complications of cirrhosis. I. Portal hypertension. *J Hepatol* 2000; **32**: 141-156